Inorganic Chemistry

Article

pubs.acs.org/IC

Phase Transition between Layered Tungstates and Polyoxotungstates in Aqueous Solutions

Takayuki Ban,* Toshihiro Ito, and Yutaka Ohya

Department of Chemistry and Biomolecular Science, Gifu University, Yanagido 1-1, Gifu 501-1193, Japan

Supporting Information

ABSTRACT: Aqueous sols of colloidal layered tetramethylammonium (TMA) tungstate nanocrystals were obtained by diluting an aqueous suspension of TMA polyoxotungstate precipitates. The slow evaporation of the colloidal-layered tungstate sols led to the deposition of TMA polyoxotungstate and significantly decreased the amount of layered tungstate nanocrystals. Moreover, the increase in the amount of TMA^+ in the sols also facilitated precipitation of the polyoxotungstates because of a common ion effect. Thus, the dissolution and formation of polyoxotungstate were reversible phenomena. The reaction between the dissolved species, which were formed by the dissolution of TMA polyoxotungstate, likely provided the highly water-dispersible layered tungstate nanocrystals. Furthermore, transmission electron microscopy observation suggested that the layered tungstate nanocrystals had a layer structure similar to those of H_2WO_4 and $H_2WO_4{\cdot}H_2O$, which is a layered tungstic acid.

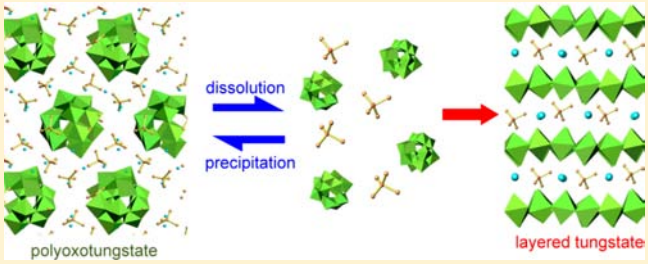

INTRODUCTION

Two-dimensional nanomaterials are attracting increasing attention because of the unusual properties dominated by their anisotropic shapes.[1,2] Metallate nanosheets are one of the interesting two-dimensional materials. When bulky quaternary ammonium ions such as $N(C_4H_9)_4^+$ are intercalated into the interlayer of layered metallic acids, the swelling of the interlayer leads to exfoliation of the metalate layers, to provide matallate nanosheets.[3] Thus, the synthesis of layered metallates with quaternary ammonium ions in the interlayer is required for the preparation of metalate nanosheets. So far, we have reported the synthesis of layered titanate,[4] niobate,[5] and tantalate[6] nanocrystals with interlayer quaternary ammonium ions by an aqueous solution process. When metal alkoxide was mixed with an aqueous solution of quaternary ammonium hydroxide and the mixture was diluted with water, then transparent aqueous sols of colloidal layered metalate nanocrystals were obtained. The acid−base reaction of metallic acids, which were formed by the hydrolysis of metal alkoxides, and quaternary ammonium hydroxides probably provided layered metalate nanocrystals. So, in the present study, this synthesis method is applied to layered tungstate. However, tungstates are prone to becoming polyoxotungstates in an aqueous solution process.[7−9] It is intriguing whether layered crystals are synthesized for metallates, which readily provide polyoxometallates.

Tungsten oxides have been studied for their chromism, photocatalysis, and sensing capabilities.[10] For tungstate nanosheets, interesting properties that are different from the properties of bulk tungsten oxides are expected.[10] Until now, tungstate nanosheets and layered tungstates were synthesized by some methods. Kalantar-zadeh et al.[11] reported the synthesis of atomically thin WO_3 sheets by the mechanical exfoliation of $H_2WO_4{\cdot}H_2O$. The obtained thin flakes had a higher propensity for lithium intercalation. Fukuda et al.[12] and Nakamura et al.[13] reported the synthesis of tungstate nanosheets, in which Cs^+ ions were included, by an aqueous solution process. Fukuda et al.[12] showed that the tungstate nanosheets have a band gap larger than that of the bulk layered precursor and exhibit highly efficient and reversible photochromic properties. Nakamura et al. also showed that the tungstate nanosheets have a larger band gap because of size quantization. Moreover, the intercalation of primary amines with a long alkyl group into layered tungstic acids H_2WO_4 and $H_2W_2O_7$ has been studied extensively.[14−17] Chen et al.[17] reported the synthesis of H_2WO_4 and WO_3 nanoplates from tungstate-based inorganic−organic hybrid materials prepared by intercalating alkylamines into layered tungstic acids and higher photocatalytic properties of the resulting WO_3 nanoplates. However, there were a few studies on the intercalation of quaternary ammonium ions[18] but none of organic amines. It is known that the acidification of an alkaline tungstate aqueous solution including the tetramethylammonium ion $[N(CH_3)_4^+; TMA^+]$ brings about the formation of TMA salts of Keggin-type polyoxotungstate, $(TMA)_6[H_2W_{12}O_{40}]{\cdot}nH_2O$ (n = 5 and 9).[7,8] The formation of polyoxotungstates may interfere with the formation of layered tungstates with interlayer quaternary ammonium ions such as TMA^+.

The purpose of this study is not only to investigate whether layered TMA tungstates are synthesized by an aqueous solution

Received: June 9, 2013
Published: August 23, 2013

dx.doi.org/10.1021/ic4014587 | Inorg. Chem. 2013, 52, 10520−10524

process but also to examine the influence of the formation of polyoxotungstates on the formation of layered tungstates.

EXPERIMENTAL PROCEDURE

Synthesis. TMA tungstate sols were synthesized by adding a diluted tetraalkylammonium hydroxide (TMAOH) aqueous solution (20 mL) to a H_2WO_4 aqueous suspension (20 mL) and then stirring at room temperature for 2 weeks. The TMAOH/H_2WO_4 molar ratio, which is designated as R hereafter, was adjusted to 0.4−2.0. The W concentration was 0.05−0.4 M. Some samples were prepared by diluting an aliquot of the suspensions with high W concentration (0.4 M). Moreover, when $N(CH_3)_3$ was used instead of TMAOH, aqueous mixtures of H_2WO_4 and $N(CH_3)_3$ were stirred at room temperature for 1 day and then were allowed to stand in an oven at 70 °C for 1 week. The $N(CH_3)_3/H_2WO_4$ ratio and the W concentration were 0.6 and 0.1 M, respectively.

Characterizations. Dynamic light scattering (DLS) measurements of the aqueous colloidal sols of layered tungstate nanocrystals were performed using an argon laser on a Malvern Zetasizer Nano ZS spectrometer. Data analysis was performed using non-negative least-squares methods.

X-ray diffraction (XRD) measurements were performed using a Rigaku Ultima IV diffractometer with monochromatic Cu Kα irradiation. XRD patterns were obtained at a scan rate of 2° min^{-1} in the 2θ range of 2−70°. XRD measurements were conducted for the thin films prepared by evaporating about 100 μL of the tungstate sols on a glass substrate (Corning no. 1737, 10 mm × 40 mm). Evaporation of the tungstate sols was carried out under an air flow at 25 °C, unless otherwise stated.

Thermal analysis (TG-DTA) was conducted on Shimadzu models TGA-50 and DTA-50. The sample powder was prepared by adding 2-propanol to the tungstate sols in order to precipitate the layered tungstate nanocrystals. After washing with 2-propanol, about 10 mg of the resulting powder was used for the measurement. TG-DTA curves were recorded under an air flow (50 mL min^{-1}) in the temperature range from 25 to 800 °C at a heating rate of 5 °C min^{-1}.

Transmission electron microscopy (TEM) images were captured using a JEOL model JEM-2100 at an accelerating voltage of 200 kV. The samples were prepared by evaporating a drop of the tungstate sols with a W concentration of 0.2−2 mM on a copper grid supported with a Formvar thin film. The copper grids were hydrophilically treated on a JEOL model HDT-400 before the use.

RESULTS AND DISCUSSION

Synthesis of Aqueous Sols of Colloidal-Layered Tungstate Nanocrystals. Aqueous sols of TMA tungstate at R = 0.5 were prepared by diluting 0.4 M sols to different W concentrations. Figure 1a shows the appearance of the sols thus obtained. The sols were opaque at W concentrations higher than 0.1 M, whereas dilution to W concentrations lower than 0.05 M brought about the dissolution of precipitates to provide transparent sols. The pH of the sol at 0.05 M was 5.6. DLS measurement showed that the sol at 0.05 M contained two types of particles: one was smaller than 10 nm, and the other had a particle size ranging from 10 to 100 nm (Figure 1b).

XRD measurements were made for the thin films prepared by evaporating the TMA tungstate aqueous sols on a glass substrate under an air flow (Figure 2). For the sample prepared from the 0.4 M sol, almost all of the peaks were assigned to a TMA salt of Keggin-type polyoxotungstate $(TMA)_6[H_2W_{12}O_{40}]\cdot 9H_2O$[8] (JCPDS 88-2061). With decreasing W concentration of the aqueous sols, the peaks assigned to the polyoxotungstate became weaker. Other than polyoxotungstate peaks with negligible intensity, the sample prepared from the transparent sols (0.05 and 0.02 M) exhibited peaks with d spacings of 1.16, 0.58, 0.39, 0.29, and 0.19 nm. These peaks were not assigned to the known TMA polyoxotungstates, i.e., $(TMA)_6[H_2W_{12}O_{40}]\cdot nH_2O$ (n = 2, 5, and 9).[7−9] Their d spacings had a relationship of $1:{}^1/_2:{}^1/_3:{}^1/_4:{}^1/_6$. This suggests that the transparent sols contained colloidal-layered tungstate nanocrystals.

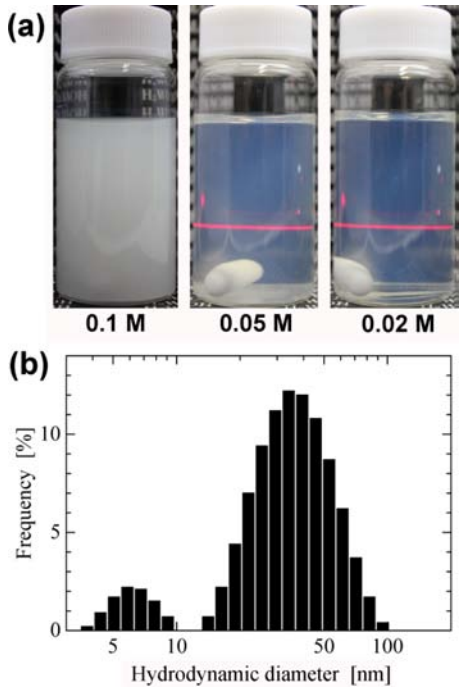

Figure 1. (a) Appearance of aqueous mixtures prepared at R = 0.5 at different W concentrations and (b) DLS results of the aqueous sol prepared at 0.05 M.

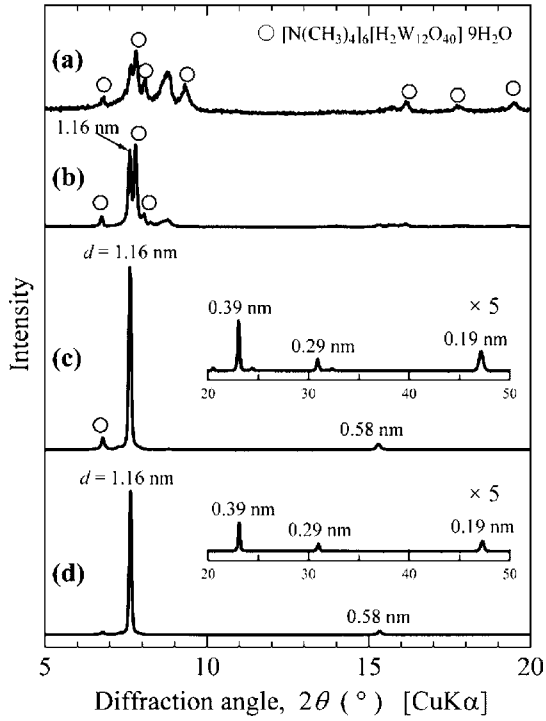

Figure 2. XRD patterns of the thin films fabricated by evaporating the aqueous mixtures prepared at R = 0.5 at different W concentrations [(a) 0.4, (b) 0.1, (c) 0.05, and (d) 0.02 M].

dx.doi.org/10.1021/ic4014587 | Inorg. Chem. 2013, 52, 10520−10524

The influence of the evaporation rates of the transparent sols on the deposited crystalline phases was investigated. The transparent aqueous sols prepared by stirring aqueous mixtures at R = 0.5 at 0.05 M for 2 weeks were evaporated on a glass substrate at two different rates: (1) rapid evaporation under an air flow and (2) slow evaporation in a loosely covered vessel. Their XRD patterns are shown in Figure S1 in the Supporting Information (SI). The sample prepared by rapid evaporation showed strong peaks of layered TMA tungstates, as mentioned above; however, slow evaporation provided a highly (100)-oriented thin film of TMA polyoxotungstate $(TMA)_6[H_2W_{12}O_{40}]\cdot 9H_2O$. Thus, the dissolution of TMA polyoxotungstate by diluting the aqueous suspensions and the deposition of TMA polyoxotungstate by slowly evaporating the transparent sols were reversible thermodynamic phenomena. When the W concentration of the TMA tungstate aqueous sols was lower than the solubility of TMA polyoxotungstate, the reaction of dissolved species probably resulted in the formation of colloidal-layered tungstate nanocrystals.

In order to confirm that the reaction of the species formed by dissolving TMA polyoxotungstate provides colloidal-layered tungstate nanocrystals, TMA polyoxotungstate was synthesized according to the literature[8] and then dissolved in water. XRD measurements were conducted for the sample prepared by evaporating the thus-obtained aqueous sols on a glass substrate. The XRD patterns of the synthesized polyoxotungstate and the sample prepared by evaporating the aqueous sol of the polyoxotungstate are shown in Figure S2 in the SI. The synthesized polyoxotungstate powder was more difficult to dissolve than the polyoxotungstate precipitates in the above-mentioned 0.4 M sols. The synthesized polyoxotungstate sample contained no layered tungstate. However, the sample prepared by evaporating the aqueous sol of the polyoxotungstate was a mixture of the polyoxotungstate and layered tungstate with a basal spacing of 1.16 nm. This confirmed that the reaction of the species formed by dissolving TMA polyoxotungstate resulted in the formation of layered tungstate nanocrystals.

The influence of the $TMAOH/H_2WO_4$ ratio, R, on the synthesis of colloidal-layered tungstate nanocrystals was examined. Aqueous sols were prepared at 0.05 M in the R range of 0.4−2.0. At R = 0.4, the sample remained a yellowish suspension even after 2 weeks of stirring. The yellow color was attributed to H_2WO_4 powder, indicating that unreacted H_2WO_4 powder was included. At R = 0.5 and 0.6, transparent sols were obtained. At R = 0.8 and 1.0, stirring for 1 week provided transparent sols; however, the sols became translucent by prolonged stirring. At R = 1.5 and 2.0, transparent solutions that did not exhibit Tyndall phenomena were obtained. The pH values of the aqueous sols at R = 0.5, 0.8, 1.0, and 1.5 were 5.6, 6.8, 7.1, and 7.6, respectively. Furthermore, XRD measurements were made for the thin films prepared from these sols (Figure 3). At R = 0.4, the sample was a mixture of unreacted H_2WO_4 and layered TMA tungstate. In the R range of 0.5−1.0, mixtures of layered TMA tungstate and TMA polyoxotungstate $[(TMA)_6[H_2W_{12}O_{40}]\cdot 9H_2O]$ were obtained. The amount of TMA polyoxotungstate increased with the R value. Interestingly, the crystallographic direction of the TMA polyoxotungstate changed from (100) to (110) orientation with increasing R values. However, we had no idea why such an orientation change occurred. At R = 1.5 and 2.0, $(TMA)_2WO_4\cdot 1.5H_2O$ formed, which is neither a polyoxotungstate nor a layered tungstate. Thus, the amount of layered tungstate nanocrystals

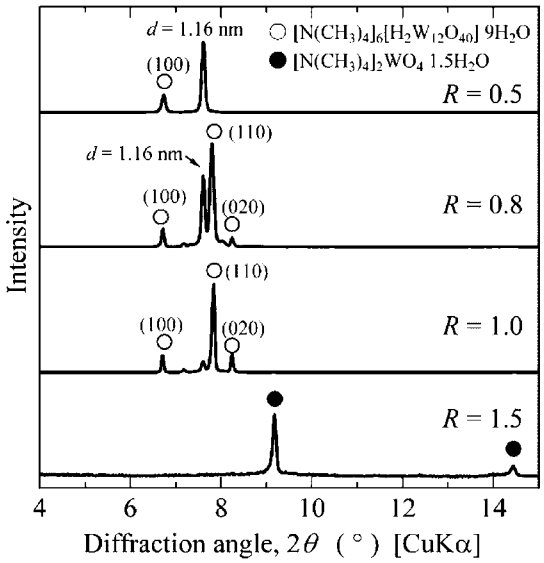

Figure 3. XRD patterns of the thin films fabricated by evaporating the aqueous mixtures prepared at a W concentration of 0.05 M at different R ratios.

was the largest at R = 0.5. At R > 0.5, the precipitation of polyoxotungstates retarded the formation of layered tungstate. A large amount of TMA^+ may facilitate the precipitation of TMA polyoxotungstate because of a common ion effect. These results also suggest that the dissolution and precipitation of TMA polyoxotungstate were reversible thermodynamic phenomena, and the reaction of the dissolved species, which were formed by the dissolution of TMA polyoxotungstate, led to the formation of colloidal-layered tungstate nanocrystals. Moreover, even when the mixture at R = 0.45 was stirred for a prolonged period (e.g., for 1 month) or heated at 70 °C for 1 week, unreacted H_2WO_4 was included in the mixture. At R = 0.5, unreacted H_2WO_4 was absent in the samples. Thus, R values larger than 0.5 was required for the formation of layered tungstate nanocrystals. At R = 0.5, a high concentration led to the precipitation of polyoxotungstates, while tungsten concentrations lower than 0.05 M resulted in an aqueous sol of layered tungstate nanocrystals. These results confirmed that the formation of layered tungstate was dependent not only on the R ratio but also on the W concentration of the sols.

Chemical Composition of Layered Tungstate Nanocrystals. In order to examine the chemical composition of the layered tungstate nanocrystals, TG-DTA maesurements were conducted for the precipitates obtained by adding 2-propanol to the aqueous sols at R = 0.5 and 0.05 M. The TG-DTA curves are shown in Figure 4. In the temperature range of 200−450 °C, two of weight losses were observed: (1) endothermic weight loss at 200−340 °C and (2) exothermic weight loss at 340−450 °C. They were likely due to the dehydration and combustion of TMA^+, respectively. Under such an assumption, the chemical composition was estimated as $(TMA)_{0.4}H_{1.6}WO_4$. Tungstic acid H_2WO_4 is a layered compound whose layers consist of vertex-sharing $WO_5(OH_2)$ octahedra. From the estimated chemical composition, it is envisaged that the obtained layered tungstate nanocrystals have a crystal structure in which part of the H^+ ions of H_2WO_4 are replaced with TMA^+. Moreover, H_2WO_4 can accommodate interlayer water molecules to provide $H_2WO_4\cdot H_2O$. Li et al.[19] reported that, upon heating $H_2WO_4\cdot H_2O$, the interlayer water molecules were

dx.doi.org/10.1021/ic4014587 | Inorg. Chem. 2013, 52, 10520−10524

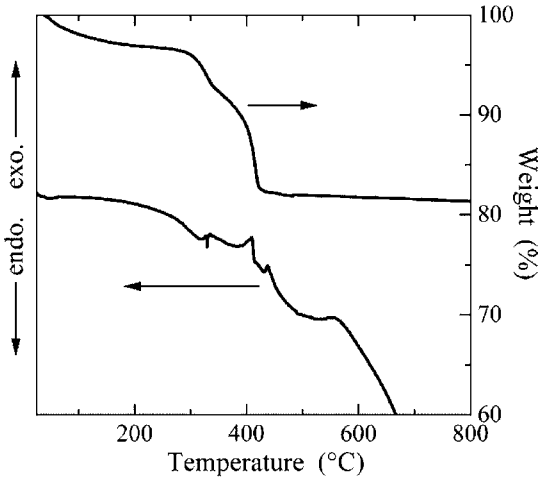

Figure 4. TG-DTA curves of layered tungstate nanocrystals.

removed at a low temperature of about 70 °C. Assuming that the weight loss below 200 °C in Figure 4 was due to the dehydration of interlayer water molecules, the chemical composition of the layered tungstate nanocrystals was estimated as $(TMA)_{0.4}H_{1.6}WO_4{\cdot}0.5H_2O$. Thus, there was the possibility that the layered tungstate nanocrystals had interlayer water molecules. The TG-DTA results suggest that the layered tungstate nanocrystals had a layered structure similar to those of H_2WO_4 and $H_2WO_4{\cdot}H_2O$, and the amount of the interlayer water molecules was smaller than that of $H_2WO_4{\cdot}H_2O$ because of the bulkiness of the interlayer TMA^+ ions.

TEM Observation of Layered Tungstate Nanocrystals. TEM observation was conducted for layered tungstate nanocrystals. Figure 5 shows the TEM images and the selected area electron diffraction (SAED). Two types of particles were observed: (1) particles smaller than 10 nm (Figure 5a) and (2) larger aggregates (Figure 5d). This was consistent with the DLS results shown in Figure 1b. The larger particles shown in the DLS results were aggregates of the small layered tungstate nanocrystals. Moreover, the transparency at $R = 0.6$ was a little higher than that at $R = 0.5$, indicating a decrease in the number of larger particles. Likely, the formed layered tungstate nanocrystals were not completely dispersed because of a little lower basicity. For comparison, the scanning electron microscopy (SEM) and TEM images of the H_2WO_4 powder used as a starting material are shown in Figure S3 in the SI.

Lattice fringes were observed in the high-magnification images of layered tungstate nanocrystals. The intervals of the lattice fringes were 0.21 and 0.38 nm for small particles and large aggregates, respectively. Because TG-DTA measurements suggested that layered tungstate nanocrystals had a layered structure similar to that of $H_2WO_4{\cdot}H_2O$, these lattice fringes were analyzed using the lattice constants of $H_2WO_4{\cdot}H_2O$ (a = 1.048 nm, b = 1.380 nm, c = 1.057 nm, β = 91.04°;[19] the tungstate layers are stacked up along the b axis) and the d spacing obtained in Figure 2. As a result, the lattice fringes of 0.21 and 0.38 nm were assigned to the (501) and (202) planes, respectively. The SAED patterns, that is, both diffraction spots from the large aggregates and diffraction rings from the small particles, were also indexed using the lattice constants a and c of $H_2WO_4{\cdot}H_2O$, as shown in parts c and f of Figure 5. These results support the similarity in the layer structure between layered tungstate nanocrystals and $H_2WO_4{\cdot}H_2O$. Thus, the crystal structure of layered tungstate nanocrystals is probably similar to the one shown in Figure 6. Furthermore, the zone axis of both SAED patterns was the [010] direction. This indicates that the layered tungstate nanocrystals were present with the tungstate layers parallel to the surface of the grids. Despite the fact that the small particles and the large aggregates consisted of the same compound and had the same orientation of tungstate layers, they provided lattice fringes with different intervals. We speculate that the number of stacked tungstate layers might have an influence on the difference in lattice fringes.

TEM observation was also conducted for tungstate nanocrystals synthesized using $N(CH_3)_3$ instead of TMAOH.

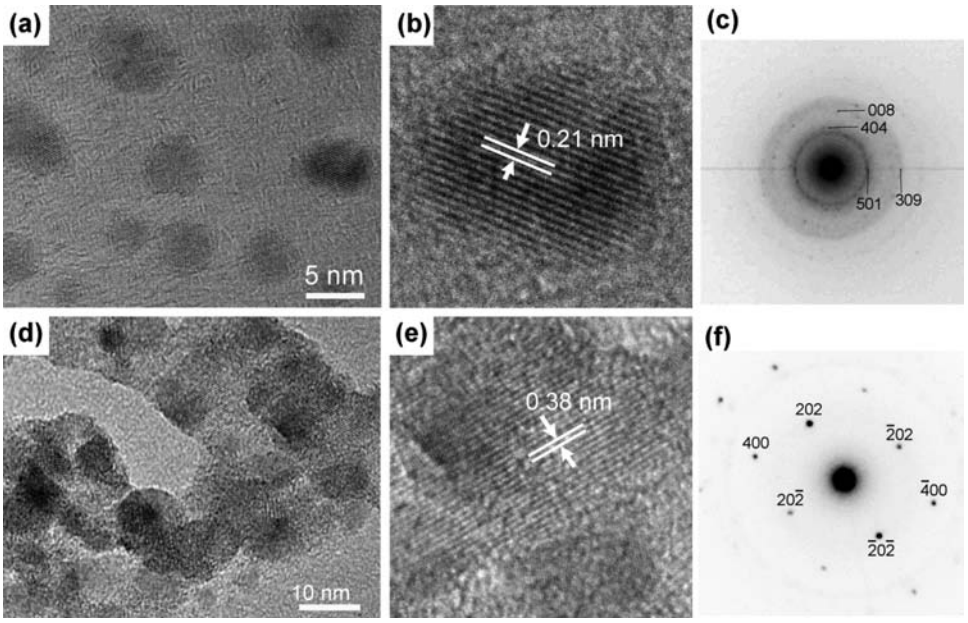

Figure 5. (a and b) TEM images and (c) the SAED pattern of layered tungstate nanocrystals and (d and e) TEM images and (f) the SAED pattern of their large aggregates.

dx.doi.org/10.1021/ic4014587 | Inorg. Chem. 2013, 52, 10520−10524

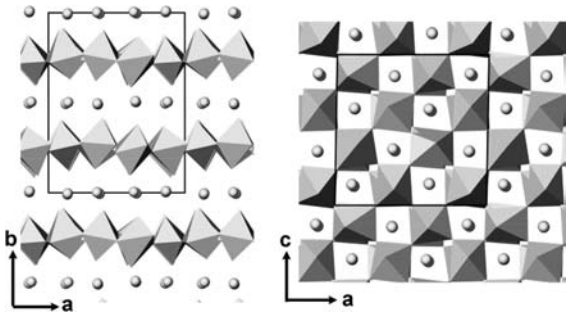

Figure 6. Crystal structure of $H_2WO_4{\cdot}H_2O$. The octahedra and circles represent $WO_5(OH_2)$ and H_2O, respectively. For layered tungstate nanocrystals, part of the interlayer water molecules are replaced with TMA^+ ions and a part of the $WO_5(OH_2)$ octahedra become $WO_5(OH)$.

Tungstate nanocrystals synthesized using $N(CH_3)_3$ also likely had a layered structure (Figure S4 in the SI), although the *d* spacing of the peaks, that is, the interlayer interval, was different from that in the case using TMAOH. The TEM images and SAED patterns of layered tungstate nanocrystals synthesized using $N(CH_3)_3$ are shown in Figure S5 in the SI. Only particles smaller than 10 nm were observed. The high-magnification images showed a lattice fringe with an interval of 0.21 nm on the small particles, which was similar to that in the case using TMAOH. The *d* spacings of the SAED ring pattern were also the same as those of the small particles synthesized using TMAOH. If tungstate nanocrystals synthesized using TMAOH and $N(CH_3)_3$ were polyoxotungstates and not a layered tungstate, the TEM images and SAED patterns should show lattice fringes with different intervals and a ring pattern with different *d* spacings, respectively. Thus, on the basis of a comparison of the tungstate nanocrystals synthesized using TMAOH with those using $N(CH_3)_3$, it is concluded that tungstate nanocrystals have a layered structure.

The WO_6 octahedra in the polyoxotungstate share a vertex with two neighboring octahedra and an edge with two other neighboring octahedra. On the other hand, the WO_6 octahedra in the layered tungstate share a vertex with four neighboring octahedra (Figure 6). Thus, there is little similarity in the crystal structure between the polyoxotungstate and layered tungstate. Probably, only the solubility of the polyoxotungstate influenced the formation of layered tungstate.

CONCLUSION

Despite the fact that tungstates are prone to becoming polyoxotungstates in an aqueous solution process, layered tungstate nanocrystals with bulky TMA^+ cations in the interlayer were synthesized. Until now, we reported that layered titanate, niobate, and tantalate nanocrystals with interlayer alkylammnonium cations were obtained as highly water-dispersible colloids by reacting metal alkoxide with TMAOH in water. Similarly, layered tungstate nanocrystals were obtained as colloids dispersed in transparent aqueous sols. However, layered tungstate nanocrystals were synthesized only under limited conditions. At a high concentration, the formation of polyoxotungstates was dominant. Only when polyoxotungstates were dissolved in water did the reaction between the dissolved species provide layered tungstate nanocrystals. Because a TMA salt of polyoxotungstate was deposited during concentration, the stabilization of layered tungstate nanocrystals would be required for utilizing the colloidal aqueous sols, e.g., for the preparation of tungstate nanosheets by exfoliation.

ASSOCIATED CONTENT

Supporting Information

XRD patterns of the thin films fabricated by the rapid evaporation and slow evaporation of aqueous sols of layered tungstate nanocrystals, XRD patterns of the synthesized TMA polyoxotungstate and the thin film fabricated by evaporating the aqueous sol prepared by dissolving the synthesized polyoxotungstate in water, SEM and TEM images and SAED pattern of the H_2WO_4 powder used as a starting material, XRD pattern of the thin film fabricated by evaporating the aqueous sols prepared using $N(CH_3)_3$, and TEM images and SAED pattern of the layered tungstate nanocrystals synthesized using $N(CH_3)_3$. This material is available free of charge via the Internet at http://pubs.acs.org.

AUTHOR INFORMATION

Corresponding Author

*E-mail: ban@gifu-u.ac.jp. Phone: +81 58 293 2585.

Notes

The authors declare no competing financial interest.

ACKNOWLEDGMENTS

This study was supported by the Asahi Glass Foundation.

REFERENCES

(1) Butler, S. Z.; Hollen, S. M.; Cao, L.; Cui, Y.; Gupta, J. A.; Gutiérrez, H. R.; Heinz, T. F.; Hong, S. S.; Huang, J.; Ismarch, A. F.; Johnston-Halperin, E.; Kuno, M.; Plashnitsa, V. V.; Robinson, R. D.; Ruoff, R. S.; Salahuddin, S.; Shan, J.; Shi, L.; Spencer, M. G.; Terrones, M.; Windl, W.; Goldberger, J. E. *ACS Nano* **2013**, *7*, 2898.

(2) Balendhran, S.; Walia, S.; Nili, H.; Ou, J. Z.; Zhuiykov, S.; Kaner, R. B.; Sriram, S.; Bhaskaran, M.; Kalantar-zadeh, K. *Adv. Funct. Mater.* **2013**, http://dx.doi.org/10.1002/adfm.201300125.

(3) Ma, R.; Sasaki, T. *Adv. Mater.* **2010**, *22*, 5082.

(4) Ohya, T.; Nakayama, A.; Ban, T.; Ohya, Y.; Takahashi, Y. *Chem. Mater.* **2002**, *14*, 3082.

(5) Ban, T.; Yoshikawa, S.; Ohya, Y. *J. Colloid Interface Sci.* **2011**, *364*, 85.

(6) Ban, T.; Yoshikawa, S.; Ohya, Y. *CrystEngComm* **2012**, *14*, 7709.

(7) Hodorowicz, E. K. *Acta Chim. Hung.* **1988**, *125*, 839.

(8) Asami, M.; Ichida, H.; Sasaki, Y. *Acta Crystallogr.* **1984**, *C40*, 35.

(9) Zavalij, P.; Guo, J.; Whittingham, M. S.; Jacobson, R. A.; Pecharsky, V.; Bucher, C. K.; Hwu, S.-J. *J. Solid State Chem.* **1996**, *123*, 83.

(10) Zheng, H.; Ou, J. Z.; Strano, M. S.; Kaner, R. B.; Mitchell, A.; Kalantar-zadeh, K. *Adv. Funct. Mater.* **2011**, *21*, 2175.

(11) Kalantar-zadeh, K.; Vijayaraghavan, A.; Ham, M.-H.; Zheng, H.; Breedon, M.; Strano, M. S. *Chem. Mater.* **2010**, *22*, 5660.

(12) Fukuda, K.; Akatsuka, K.; Ebina, Y.; Ma, R.; Takada, K.; Nakai, I.; Sasaki, T. *ACS Nano* **2008**, *2*, 1689.

(13) Nakamura, K.; Oaki, Y.; Imai, H. *J. Am. Chem. Soc.* **2013**, *135*, 4501.

(14) Chen, D.; Li, T.; Yin, L.; Hou, X.; Yu, X.; Zhang, Y.; Fan, B.; Wang, H.; Li, X.; Zhang, R.; Hou, T.; Lu, H.; Xu, H.; Sun, J.; Gao, L. *Mater. Chem. Phys.* **2011**, *125*, 838.

(15) Chen, D.; Sugahara, Y. *Chem. Mater.* **2007**, *19*, 1808.

(16) Wang, B.; Dong, X.; Pan, Q.; Cheng, Z.; Yang, Y. *J. Solid State Chem.* **2007**, *180*, 1125.

(17) Chen, D.; Gao, L.; Yasumori, A.; Kuroda, K.; Sugahara, Y. *Small* **2008**, *4*, 1813.

(18) Schaak, R. E.; Mallouk, T. E. *Chem. Commun.* **2002**, 706.

(19) Li, Y. M.; Hibino, M.; Miyayania, M.; Kudo, T. *Solid State Ionics* **2000**, *134*, 271.